

"Never be afraid to raise your voice for honesty and truth and compassion against injustice and lying and greed." -William Faulkner

2024 National Scholarly Press

December / January, 2024 Volume One / Issue One

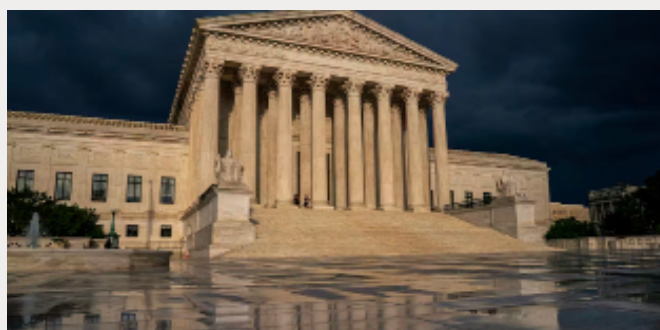
Innovation

Martian Ionosphere 1

Economy/Business

Sports

Social Studies



Stay Active * Raise Voices * Be Motivated

Innovation

Identification and Statistics of Martian Nightside Ionosphere

By Haiming Xu

Abstract:

The ionosphere, a partially charged atmospheric layer between 80–600 km on Earth, is crucial for communication and navigation, as its ions and electrons affect radio wave propagation. However, variability in solar radiation and magnetic fields causes constant changes in its composition, leading to signal distortion and delays. Understanding and monitoring the ionosphere is essential for military operations, GPS, and GNSS systems. Research on exoplanet ionospheres, particularly Mars, has gained attention due to their importance in space communication and planetary studies. Mars' ionosphere, first confirmed by Mariner 4, is vital for understanding atmospheric loss, climate evolution,

Introduction:

Introduction to the Martian Ionosphere

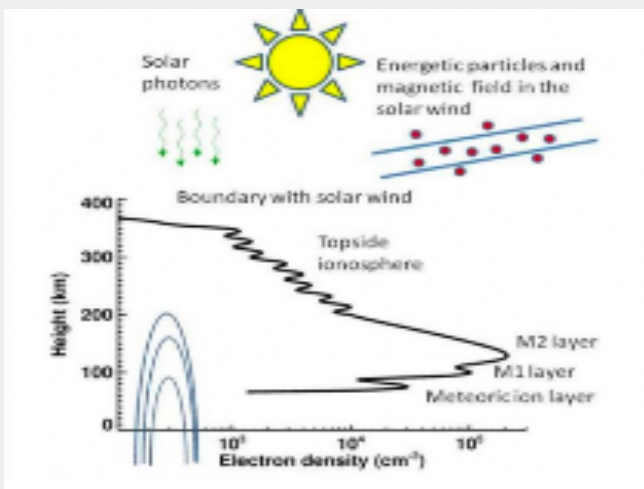


Figure 1.1 the illustration of Martian Ionosphere

The Martian ionosphere, spanning 80–400 km, is a partially ionized region containing free electrons and ions such as O^+ , O_2^+ , and CO_2^+ . Its formation is driven by extreme ultraviolet (EUV) radiation and collisions between high-energy particles and neutral gases like CO_2 , Ar, and N_2 . The ionosphere's stability is influenced by gravitational forces, chemical reactions, transport processes, and plasma

instabilities, with weaker planetary gravity leading to less stable ionospheres.

The ionosphere comprises distinct layers (Figure 1.1):

- **M1 Layer (100–120 km):** Formed by EUV-induced photoionization of CO_2 , with electron density peaking where EUV intensity and CO_2 concentration are highest. Solar activity drives fluctuations in its electron density.
- **M2 Layer (120–150 km):** Created by EUV and X-ray radiation, which penetrate deeper, making it the peak electron density region. Its properties also vary with solar activity.
- **Meteoroid Layer (70–100 km):** A transient layer caused by meteoroid ablation, releasing ions and electrons. Its effects, though short-lived, significantly influence ionospheric behavior.

The Martian ionosphere displays a dichotomy:

- **Dayside Ionosphere:** Stabilized by solar radiation (X-rays and UV), with photochemical processes dominating. It features high electron density and conductivity, essential for communication systems.
- **Nightside Ionosphere:** Highly variable, shaped by solar energetic particles (SEPs) and plasma transport from the dayside. Factors such as solar zenith angle (SZA), local solar time (LST), and solar activity cycles influence its unstable electron density.

While the dayside ionosphere is well-studied, the nightside remains less understood. The relationship between ionospheric variability and factors like SZA, latitude, and LST requires further investigation.

Summary of 2.2

2.2.1 Influence of Local Magnetic Field

The Martian nightside ionosphere is significantly affected by localized magnetic fields originating from “remanent magnetism.” These magnetic fields were formed when ancient Martian rocks, rich in iron, were magnetized by a now-extinct global magnetic field generated by a liquid iron-nickel core. Volcanic activity, including eruptions from shield volcanoes like Olympus Mons, also contributed to localized magnetic fields as cooling lava retained magnetic information.

2.2.2 Meteoroid Impact and Magnetic Enhancement

Large meteoroid impacts generate intense heat, melting and re-magnetizing nearby rocks. Shock waves can rearrange magnetic minerals, enhancing localized magnetic fields. These ancient impacts, along with volcanic activity, are key contributors to Mars' current localized magnetic anomalies.

2.2.3 Solar Wind Interaction with Magnetic Fields

The solar wind, a plasma stream from the Sun, interacts with Mars' localized magnetic fields, influencing the nightside ionosphere. The solar wind carries the interplanetary magnetic field (IMF) and interacts with Mars' crustal fields, shaping plasma behavior. This interaction leads to changes in electron density and can drive abnormal ionospheric activity.

2.2.4 Magnetic Spikes and Ionization

Mars exhibits magnetic spikes or cusps, which allow solar wind particles to enter the atmosphere, causing ionization and excitation of neutral molecules. This process increases electron density, forming auroral regions similar to Earth's. Conversely, regions with horizontal magnetic fields lack significant ionization, creating plasma voids.

2.2.5 Particle Collisions

Collisions between particles in the ionosphere are categorized as:

- Elastic Collisions: Minor energy transfer, affecting particle motion but not ionization.
- Inelastic Collisions: Significant energy loss, driving ionization and excitation of molecules. Secondary electrons from collisions contribute to chain reactions, increasing local electron density.

2.2.6 Temperature and Conductivity

Enhanced conductivity in the ionosphere creates stronger currents and electric fields, which increase particle collisions and ionization. Joule heating from these currents raises local temperatures, boosting ionization rates and reducing recombination rates, further increasing electron density.

2.2.7 Solar Zenith Angle (SZA)

The SZA, the angle between the Sun's rays and the zenith, influences ionospheric behavior. Larger SZAs on the nightside reduce solar radiation, weakening ionization and increasing recombination, leading to lower electron densities. However, at high altitudes, diffused electrons from the dayside sustain some ionization.

2.2.8 Solar Activity

Solar activity, including solar wind, coronal mass ejections (CMEs), and flares, impacts the nightside ionosphere. CMEs inject high-energy particles into Mars' magnetotail, causing ionization and increasing electron density. Compression effects from solar wind and CMEs enhance local magnetic fields and plasma density, altering ionospheric structure and behavior.

Expanded 2.2 Influencing Factors of TEC in the ionosphere

2.2.2 Meteoroid Impact and Local Magnetic Field Enhancement

Meteoroid impact is another factor. Large meteorite impact event generates enough heat to melt the rock around the impact point. These molten rocks were re-magnetized by the magnetic field at that time, and the shock waves from an impact point may have rearranged the magnetic minerals in the rock, thereby enhancing local magnetic fields. Mars' local magnetic field therefore is the result of the residual effects of these ancient, magnetized rocks, along with other effects such as volcano activities and geographic transformation.

2.2.3 Solar Wind and Its Interaction with Local Magnetic Field

The local magnetic field could influence the behavior of solar wind, leading to abnormal phenomena in the Martian nightside ionosphere. The solar wind, a stream of plasma ejected outward from the sun's hot corona. Travels at a speed usually between 300 and 800 kilometers per second. The density of solar wind decreases with distance from the sun, carrying particles like protons, electrons, and alpha particles, along with small amounts of other ions, such as oxygen, carbon,

and nitrogen. their small particles would interact with Mars's localized magnetic fields, which in turn play a critical role in shaping the nightside ionosphere.

Additionally, the solar wind carries a Magnetic Field originating from the sun called the Interplanetary Magnetic Field (IMF), featuring a spiral-shaped magnetic field known as the Parker Spiral, resulting from the rotation of the sun and the radial propagation of the solar wind. The direction and strength of the IMF vary with the solar cycle, with a typical magnetic field strength of about 5 nanoteslas (nT) at Mar's orbit.

2.2.4 Magnetic Spikes and Solar Wind Electron Interaction

Mars is characterized by numerous magnetic spikes, also known as magnetic cusps, regions where the planetary magnetic field is connected with the interplanetary space, allowing the charged particles to precipitate or escape from the planet (in situ evidence of the magnetosphere cusp of Jupiter). Upon the entry of solar wind particles, these high-energy electrons will collide with neutral molecules in the atmosphere (such as CO₂, N₂, O₂, etc.), resulting in an increase in electron and ion density in the local ionosphere through Ionization and Excitation reaction shown in Figure 1.2 and 1.3.

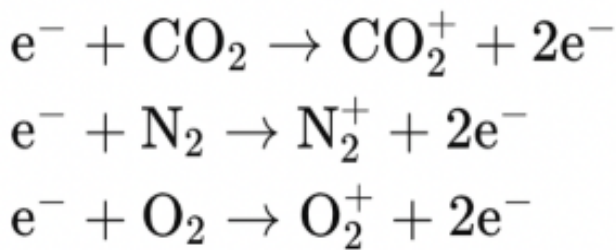


Figure 1.2 Ionization reaction: High-energy electrons collide with neutral molecules, causing the molecules to ionize, forming positive ions and free electrons.

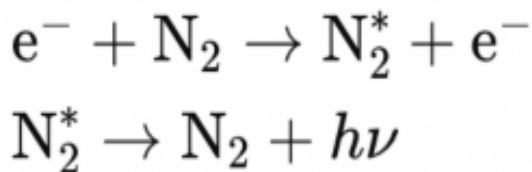


Figure 1.3 Excitation reaction: High-energy electrons also put neutral molecules in excited states, which return to the ground state by releasing photons, creating an aurora.

As a result, these regions are usually accompanied by the presence of strong currents and electric jets, similar to regions on Earth where auroras occur. Furthermore, these magnetic spike regions are particularly pronounced on the nightside ionosphere, which causes significant ionization enhancement and local current formation compared to the dayside ionosphere (M. O. Fillingim, 2012). Conversely, in areas where the crustal magnetic fields are horizontal, the solar wind electrons are unable to penetrate the atmosphere, leading to a lack of ionization and the presence of plasma voids. (M. O. Fillingim, 2012)

2.2.5 Particles Collisions

Particles collisions can be categorized into two major types of collision: elastic and inelastic collisions

- **Elastic Impact:** In an elastic collision, when an electron collides with a neutral molecule, part of the kinetic energy of the electron is transferred to the neutral molecule, while the electrons retain relatively most of their energy. Such collisions primarily affect the speed and direction of motion of the electrons without significantly affecting their energy. As a result, the elastic collision has minimal impact on the ionosphere as they do not significantly alter electron density, thereby making its influence on TEC negligible.
- **Inelastic Collision:** An inelastic collision is when an electron collides with a neutral molecule and the kinetic energy of the electron is significantly reduced. The energy loss in the collision process is then used to excite or ionize the neutral molecules. This type of collision plays a critical role in driving the chemical reactions that substantially alter the TEC in the nightside ionosphere. Inelastic collisions are the principal contributor to changes in TEC due to the ionization and excitation processes they initiate.

Furthermore, the secondary electrons produced by the collision of the primary electrons retains high energies, and these secondary electrons will continue to collide with other neutral molecules, triggering even more ionization reactions. This secondary reaction also functions by increasing the electron density and conductivity of the local region. There is an energy decline during the reactions.

Each step of ionization dissipates the energy of the electrons further, eventually reducing the energy of the electrons to a level that is not sufficient to cause ionization again. This energy decline process continues throughout the electron deposition until the electron has completely exhausted its energy or is absorbed by the atmosphere. Besides, as the elastic impact, the tubes transfer only a small amount of energy per collision, but because electrons undergo a large number of elastic collisions in the atmosphere, the cumulative effect causes the energy to dissipate gradually. This energy transfer is a gradual process and also plays an important role in the overall energy dissipation. Due to the chain reaction, the regions near the magnetic tip, their local TEC will be increased.

2.2.6 Temperature and Electric Conductivity

The increase in conductivity enhances the currents in the ionosphere, which create a horizontal electric field in response to a magnetic field. The enhancement of the electric field will change the trajectory of charged particles in the ionosphere, making the electrodynamic behavior of the ionosphere more complicated. And a very important way is that an increase in conductivity leads to an increase in current, and the Joule heating effect occurs when current passes through the ionosphere. This heating increases local ionospheric temperatures and changes the dynamics of the atmosphere. Besides, not only the currents can make the local regions get the heat, but also the local regions will be heated by the heat from direct kinetic energy conversion. The kinetic energy of high-energy electrons is directly converted into heat energy in the elastic collision with atmospheric molecules. Although the energy transfer of a single collision is small, the cumulative effect is significant. As a result, some local region's temperature will be enhanced. The increasing of local region's temperature will have a strong influence on the martian nightside ionosphere. First, Temperature and ionization rate will significantly increase collision frequency. Since the local temperature increase directly affects the kinetic energy of the particles. According to kinetic theory, temperature is proportional to the average kinetic energy of particles.

$$\frac{3}{2}k_B T = \frac{1}{2}mv^2$$

Figure 1.4 k_B : Boltzmann's constant; T : Temperature; m : Mass of particle; v : The average velocity of a particle.

An increase in temperature causes the average velocity of particles to increase, which increases the frequency of collisions between particles. High-energy electrons collide more frequently with neutral molecules in the atmosphere, leading to more ionization reactions. These ionization reactions produce more positive ions and free electrons, directly increasing the electron density of the ionosphere. And the increase in temperature not only increases the collision frequency of primary electrons, but also increases the production of secondary electrons. These secondary electrons also have high kinetic energy and can continue to collide with neutral molecules, leading to further ionization reactions.

It will also enhance the secondary ionization. The secondary electrons produced by the primary ionization reaction have higher kinetic energy in the high-temperature environment. These high-energy secondary electrons will further collide with neutral molecules in the atmosphere, resulting in an increased frequency of secondary ionization reactions. This secondary ionization reaction is not only a continuation of the primary ionization reaction, but also significantly increases the electron density in the local region. The enhancement of secondary ionization creates a chain reaction that significantly increases the electron density in a local region. This reaction process results in an exponential increase in electron density, especially in regions where high-energy electron deposition and local temperature rise are significant.

The increase of temperature will not just impact the rate of ionization, it can also affect the rate of recombination. It is also a vital factor for the change of the martian nightside ionosphere. The recombination process is a process in which electrons and ions recombine to form neutral molecules in the ionosphere, the rate of which is significantly affected by temperature. The recombination rate is usually inversely proportional to the temperature of the electrons and ions.

Higher temperatures will reduce the recombination rate, because electrons and ions at higher temperatures have greater kinetic energy and do not easily combine to form neutral molecules.

$$\alpha(T) \propto T^{-0.5}$$

Figure 1.5 (T): Recombination Coefficient; T: Temperature

As a result, higher temperatures lead to a lower recombination rate, which in turn reduces the recombination of electrons and ions, meaning that more electrons will remain in the ionosphere, increasing electron density.

2.2.7 Solar Zenith Angle

Solar Zenith Angle (SZA) is an important astronomical and meteorological concept used to describe the position of the sun in the sky. Specifically, the zenith Angle of the Sun is the Angle between the sun's rays and the vertical direction at the observation point (zenith direction). When the sun is just above the observation point, the zenith Angle of the sun is 0 degrees. When the sun is at the horizon, the zenith Angle is 90 degrees. The magnitude of this Angle directly affects the intensity of solar radiation reaching the surface. And due to the calculation of the solar zenith Angle involves several parameters, including the geographical location of the observation point (longitude and latitude), the time of observation (time of day and date of year), and the characteristics of the Earth's rotation and revolution, we usually calculate the Solar Zenith Angle (SZA) by the formula:

$$\cos(\theta_z) = \sin(\phi) \sin(\delta) + \cos(\phi) \cos(\delta) \cos(h)$$

Figure 1.6 **Theta(z)**: Solar Zenith Angle (SZA);

Phi: Geographical latitude of the observation point;

Delta: The declination Angle of the sun, which varies with time;

h: Solar hour Angle, which represents the east-west position of the sun with respect to the observation point

Solar zenith Angle is an important parameter to describe the position of the sun, it is also vital to study the martian nightside ionosphere.

We can understand from the passage of introduction that during Martian day, solar radiation is the main source of electron density in the ionosphere. Solar ultraviolet (UV) and X-ray radiation ionize gas molecules (mainly carbon dioxide and nitrogen) in the Martian atmosphere, creating a large number of free electrons and ions. However, as the solar zenith Angle (SZA) increases, the intensity of solar radiation gradually decreases, resulting in a significant decrease in electron density in the nightside ionosphere of Mars. At night, the Martian ionosphere is largely dependent on the diffusion of electrons and reionization caused by high-energy particles in the ionosphere during the day. Since the nightside ionosphere depends on the electrons that transmit from the dayside ionosphere. The definition of Solar Zenith Angle is that the zenith Angle is the Angle between the sun's rays and the vertical upward direction of the horizon. Therefore when the sun is directly above the observation point, SZA is 0 degrees. When the sun is at the horizon, SZA is 90 degrees; On the night side, SZA can approach 180 degrees. The smaller the SZA, the greater the solar light intensity and the stronger the ionization effect. The larger the SZA, the smaller the solar light intensity and the weaker the ionization effect.

Actually the nature of that is in the martian nightside ionosphere without any solar radiation as the paper mentions before. The rest of the energy could not support the ionization, but it is a very good situation for the rest of the electrons to recombine. So the rate of ionization will weakened, but the rate of recombination is increasing. Therefore with the increase of the SZA, the common ionization that frequency of occurrence is the highest will decrease quickly and obviously, so the TEC also decreased, we can see this phenomenon of TEC reduced in the Figure 4 that most of TEC change is decreasing. Even if the common ionization could not continue ionizing, the frequency of abnormal actions will also be decreased.

However, there is a special situation that, at night, with the increase of SZA, the electron density of the low altitude layer decreases more significantly, while at higher altitudes (such as more than 200 km), the contribution of daytime diffusion of electrons and reionization processes to the electron density is greater, resulting in a relatively high electron density of the high altitude layer.

With the change of SZA, the local magnetic anomaly of Mars has a significant effect on the ionospheric electron density. In these regions, local magnetic fields can trap and guide high-energy particles, enhancing local ionization. This part the paper mentions in the above passage.

Solar zenith Angle (SZA) is one of the main factors in the nightside ionosphere. It impacts common ionization actions, and the abnormal ionization actions at the same time. As the solar zenith Angle increases, the less particles of solar wind sedimentation can arrive, especially the electrons, therefore the less reaction like collision ionization will occur. As a result, the holistic ionization rate will decrease. Due to that, the frequency of the abnormal ionization actions will occur. The TEC of the nightside ionosphere reduces obviously.

Like what is mentioned above, the change of martian nightside ionosphere TEC when the SZA is changing, as for its essence is the solar wind. Because the solar wind is the main energy resource for the nightside ionosphere, if the solar wind is changed the martian nightside ionosphere will have an obvious change and martian nightside ionosphere TEC is too. Therefore the solar wind is also a vital factor to the martian nightside ionosphere and to the martian nightside ionosphere abnormal actions or we can say the solar actions can affect martian nightside ionosphere.

2.2.8 Solar Activity

Solar activity refers to the energy release and phenomena of the sun on various time scales, including solar wind, sunspots, flares, coronal mass ejections, etc. Solar activity affects not only the Sun itself, but also the Earth and the entire solar system through solar wind and electromagnetic radiation. One of the main types of solar activity are sunspots, which are dark patches on the Sun's surface that appear darker due to cooler temperatures than surrounding areas. Closely related to sunspots are solar flares, which are sudden releases of energy. Flares occur in the lower part of the sun's atmosphere, between the chromosphere and the corona. Another important solar event is a coronal mass ejection (CME), which is a massive ejection of coronal plasma and magnetic fields.

The solar wind is another important form of solar activity, which is plasma in the sun's outer atmosphere, the corona, flowing outward at hundreds of kilometers per second throughout the solar system. The speed and density of the solar wind is not constant, and it is influenced by activity on the Sun's surface, such as changes in sunspots and flares. Fast solar wind tends to come from coronal holes, which are areas of the corona where the magnetic field is open. The solar wind interacts with the martian magnetic field and can have an impact on the Martian magnetosphere and ionosphere. And over longer timescales, solar activity also shows greater cyclical variations.

There are many essential reasons why solar wind can impact martian nightside ionosphere obviously. First is solar wind compression. As the solar wind travels, it interacts with a planet's magnetic field, especially on a planet with no global magnetic protection, such as Mars. When the solar wind encounters Mars, its momentum and pressure create a compression effect on the windward side of Mars. It will cause in the region where the solar wind interacts with the Martian atmosphere and local magnetic field, a magnetosphere-like structure is formed. This structure would be compressed by the pressure of the solar wind, especially if the solar wind is strong, and the Martian magnetosphere and magnetotail would compress significantly closer to the Martian surface. Then the compression effect increases the plasma density in the magnetic tail region. This increase in density can lead to more plasma and high-energy particles entering the ionosphere of Mars, including not only electrons, but also ions, both of which produce more free electrons in the ionosphere through collision and ionization processes, thus increasing the electron density, especially in the night-side region, increasing the electron density. Because the solar wind injects plasma into the nightside ionosphere of Mars through the magnetotail, this injection can significantly increase the electron density on the nightside. Besides, the compression of the solar wind also increases the strength of the local magnetic field around Mars, which further affects the movement and distribution of plasma and changes the structure and properties of the Martian ionosphere. Except the solar wind, the coronal mass ejection (CME) will also have a great influence to the mars as it is one of the most powerful bursts of solar activity and it affects martian nightside ionosphere's TEC in many ways.

First, it involves injection of high-energy particles. During CME events, a large number of high-energy particles are ejected into interplanetary space, mainly consisting of high-energy electrons, protons, and heavy ions. When the CME reaches Mars, these energetic particles quickly penetrate Mars' magnetotail region and enter its ionosphere. Since Mars has no effective shielding from a global magnetic field, these particles easily reach the Martian surface and atmosphere, especially in the night-side region. High-energy particles collide with molecules and atoms in the atmosphere, causing an ionization reaction that produces a large number of free electrons. This process directly leads to a significant increase in electron density in the night-side ionosphere.

Second, the magnetic field carried by the CME interacts with the local magnetic field of Mars. It will cause the phenomenon like the local nightside ionosphere is heated and then it will increase the TEC in those regions, especially in the time of CME events. This part I have already written in the part about the Martian nightside local magnetic field above.

Third, it is similar to the solar wind. Magnetic perturbations in CME events can cause compression and reconfiguration of the Martian magnetotail. This perturbation increases the plasma density in the magnetotail and may trigger fluctuations in electron density in the night-side ionosphere. In particular, during strong CME events, the plasma density increases more significantly in the magnetotail region, which has a direct effect on the electron density of the night-side ionosphere.

Besides, when the large amount of plasma carried in the CME reaches Mars, it significantly increases the plasma density in the Martian ionosphere. The CME's plasma cloud typically contains high-energy electrons and ions, and when these plasmas come into contact with the Martian atmosphere, they increase the number of free electrons through ionization and collision processes (a series of ionization reactions including direct, collision, and secondary ionization). In addition, the high density and high energy properties of the CME plasma make these processes more intense, resulting in a sharp increase in electron density in the night-side ionosphere.

These ionization processes not only increase the electron density of the ionosphere on the night side of Mars, but may also cause changes in the structure of the ionosphere.

3. Experimental Design

3.1.1 Data Source and Types Introduction

Mars Express, a comprehensive Mars-detecting orbiter launched in 2003, remains operational today. It can detect a variety of scientific data, including the mineral composition of the Martian surface, atmospheric composition, air temperature, pressure, and more. Due to its extensive data collection, Mars Express has significantly contributed to our understanding of Mars. Many crucial research findings are based on data obtained from this mission, although its data alone cannot provide a complete understanding of Mars.

Mars Express is equipped with advanced scientific instruments to measure a wide variety of scientific data. For example, the Mars Advanced Radar for Subsurface and Ionosphere Sounding (MARSIS), a subsurface radar sounder with 40 meters antenna on the Mars Express orbiter, is designed to map the geographic features of Mars, search for Martian surface and underground water, and study the atmospheric composition and activities. In terms of Martian ionosphere research, by sending radio waves into the Martian atmosphere and detecting the reflections, MARSIS can measure the total electron content (TEC) and the electron distribution in each ionosphere layer. Total electron content represents the total number of electrons present between the radio wave transmitter and receiver, and as the TEC is higher in the ionosphere on the path of the radio wave, the more the radio waves will be affected. The distortion of the radio wave signal will then be collected and analyzed by the MARSIS to calculate the TEC value (Total Electron Content | NOAA / NWS Space Weather Prediction Center, n.d.). This allows MARSIS to monitor the variability in the Martian ionosphere and its response to influences such as solar winds, energetic particles, and other physical processes (Hook, n.d.). In this research, we primarily use unprocessed data from Mars Express. The datasets we focus on include solar zenith angle (SZA), local solar time (LST), latitude, longitude, and total electron content (TEC) to study

the Martian nightside ionosphere. These data sets reflect not only the temporal relationship between LST and TEC but also the spatial relationship between SZA and TEC. This comprehensive approach allows us to study the Martian nightside ionosphere in as much detail as possible, thereby ensuring our conclusions are closely aligned with the actual conditions on Mars.

3.1.2 Data Preprocessing

In this experiment, data obtained from Mars Express is used. Because the data is unprocessed, it is necessary to address various forms of interference and noise. These include unrelated plasma and energetic particles from space, solar radiation affecting the instruments, signal attenuation due to communication between Mars and Earth, and inevitable electromagnetic interference from the spacecraft itself. Consequently, preprocessing is essential to filter out noise and correct erroneous data, ensuring that the information accurately reflects the real conditions of the nightside ionosphere.

Firstly, I select the required data, specifically the Total Electron Content (TEC), which represents the total number of electrons present between the radio wave transmitter and receiver, and Solar Zenith Angle (SZA), which refers to the angle between a vertical line to the Mars surface and a line pointing to the sun. In this experiment, SZA and TEC will be paid extra attention since they are the root cause of ionosphere anomalies.

Other parameters shown in Table 1 include Local Solar Time (LST), indicating time measured by Mars's rotation relative to the Sun; latitude (LAT) and longitude (Lon), which pinpoints the exact geographic location on Mars; altitude, the vertical distance of the measured layer of the ionosphere above a reference point defined as the atmospheric pressure of 6.1 millibars (or 610.5 Pascals); and J200 time, representing Julian time, a standard astronomical time format used to indicate the time for the Mars Express probe to detect relevant data. The original dataset encompasses various scientific measurements, so this step is crucial for focusing on relevant information and removing all other extraneous data. Then, I write a program to smooth the data, eliminating minor

fluctuations caused by the aforementioned factors. This program processes the original data to generate images, identify fluctuations, and determine whether these fluctuations are noise. Finally, it filters out the noise and exports the preliminarily processed data. The resulting data are organized by type, as illustrated in Figure 2.1.

J2000_Time_s	lat	lon	LST	ALT	SZA	TEC_m2
1733280015.8678952	-28.468	274.3385	18.825	353.325	180.884	1.8528e+15
1733280022.9583288	-28.475	274.3385	18.824	353.325	180.852	1.8528e+15
1733280034.2446484	-28.577	274.5926	18.824	353.322	180.871	1.8564e+15
1733280055.2328036	-28.662	274.591	18.824	352.874	180.104	1.1552e+15
1733280095.6221159	-28.746	274.592	18.825	352.726	180.137	1.2204e+15
1733280096.1185350	-28.831	274.592	18.825	352.506	180.178	1.2576e+15
1733280099.3984741	-28.916	274.594	18.826	352.416	180.203	1.2886e+15
1733280099.6481893	-27.980	279.1395	18.826	352.489	180.237	1.2392e+15
1733280099.9767616	-27.885	279.1386	18.827	352.176	180.278	1.2381e+15
1733280099.2858665	-27.178	279.1388	18.827	352.025	180.480	1.1388e+15
1733280099.3589897	-27.296	279.1389	18.828	351.917	180.456	1.8120e+15
1733280099.8328549	-27.349	279.1388	18.828	351.792	180.469	1.5111e+15
1733280097.1317549	-27.424	274.681	18.828	351.878	180.482	1.5899e+15
1733280098.4158581	-27.508	274.682	18.829	351.551	180.435	1.6193e+15
1733280099.7065253	-27.593	274.683	18.829	351.435	180.465	1.6805e+15
1733280098.9977453	-27.670	274.685	18.829	351.322	180.502	1.5801e+15
17332800912.2057085	-27.762	274.686	18.830	351.212	180.535	1.5804e+15
1733280093.5744127	-27.847	274.687	18.831	351.105	180.560	1.3327e+15
1733280094.8628257	-27.932	279.680	18.831	351.080	180.691	1.2256e+15
1733280096.1516769	-28.016	279.680	18.831	350.889	180.633	1.2214e+15
1733280097.4188881	-28.101	279.681	18.832	350.881	180.666	1.2804e+15
1733280098.7288281	-28.186	279.682	18.832	350.785	180.699	1.2988e+15
1733280098.0573813	-28.278	279.683	18.832	350.683	180.732	1.3488e+15
1733280097.8867888	-28.355	279.683	18.833	350.525	180.765	1.5458e+15
1733280097.8948188	-28.448	279.683	18.833	350.437	180.798	1.5898e+15
1733280093.8834518	-28.525	274.617	18.834	350.353	180.831	1.1775e+15
1733280095.1728670	-28.609	274.619	18.834	350.272	180.864	1.3218e+15
1733280096.4687232	-28.694	274.620	18.835	350.195	180.896	1.4168e+15
1733280097.7469362	-28.779	274.621	18.835	350.125	180.928	1.5822e+15
1733280099.0379774	-28.864	274.623	18.836	350.040	180.962	1.4267e+15
1733280098.3266116	-28.949	279.624	18.836	349.879	180.995	1.4549e+15
1733280099.6152286	-29.033	279.626	18.837	349.813	181.027	1.4531e+15
1733280099.9068818	-29.118	279.627	18.837	349.650	181.060	1.4886e+15
1733280091.1928888	-29.203	279.628	18.838	349.590	181.094	1.5358e+15
1733280093.4811248	-29.287	279.630	18.838	349.524	181.128	1.6398e+15
1733280096.7897582	-29.372	279.631	18.838	349.476	181.158	1.7491e+15
1733280098.0885954	-29.457	274.833	18.839	329.827	181.191	1.7544e+15

Figure 2.1: the table presents the data processed through the developed program, including parameters J2000 time in seconds, latitude (lat), longitude (lon), local solar time (LST), altitude (ALT), solar zenith angle (SZA), and total electron content (TEC) expressed in electrons per square meter squared (TEC_c/m^2). The data illustrate the ionospheric conditions of the Martian nightside as captured by Mars Express.

3.2 Algorithm Design and Improvement

To select the appropriate data from the unprocessed dataset, we apply the rolling barrel algorithm, which is specifically designed to recognize and eliminate the depletions in TEC time series data, data collected during the period when TEC values are significantly lower than the surrounding levels (Rezy Pradipta, 2015). Eliminating the depletions of TEC time series data is similar to filtering out the outliers in a statistical dataset, which helps us to better handle the abrupt seasonal or day-to-day variability presented in the TEC dataset and analyze the underlying trends without the influence of noises. To better understand how the algorithm works to filter the extraneous data, we can compare this algorithm to a wheel rolling along a terrain of discrete signal values (Figure 2.2).

The core concept of this algorithm involves rolling a simulated wheel along a line connected by the data point on the coordinates, generating the contact points between the wheel and the desired data point.

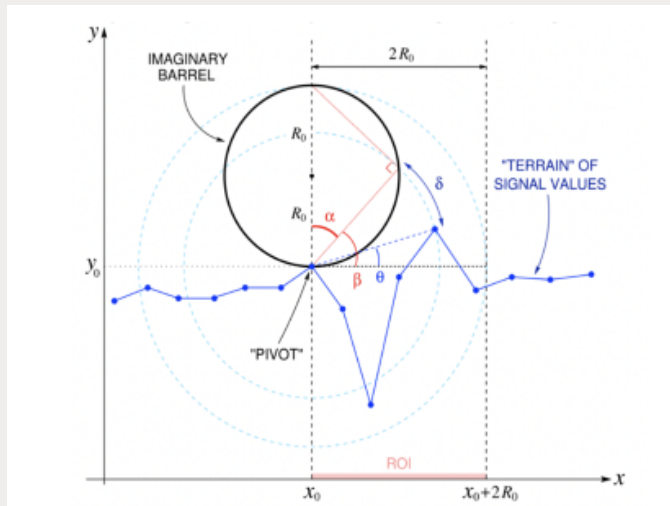


Figure 2.2 Illustration of the Wheel Rolling Barrel Algorithm on a signal terrain.

The diameter($2R_0$) defines a circular range to capture the desired data points that fall within this range and are aligned in the forward direction. The algorithm follows these steps:

1. Data Processing: Scaling and mapping the TEC time series data on the x-y coordinates. The scaling equation for time and TEC is shown below:

$$x = \frac{\text{time}(t)}{\tau_n}$$

$$y = \frac{\text{TEC}(\text{TECU})}{\zeta_n}$$

where $\tau_n = 2h$, $\zeta_n = 40$, and $1 \text{ TECU} = 10^{16} \text{ electrons/m}^2$.

2. Contact point calculation: a circle with radius $2R_0$ is drawn along the data line and roll forward until resting on a contact point and pivot around this center of rotation. Based on the geometry depicted in figure 2, we know that $\delta = \beta - \theta$, $\theta = \text{inverse tan}(\text{change in } y \text{ over change in } x)$, and $\alpha = 90 - \beta$. We first calculate the cosine of α by

$$\cos \alpha = \frac{\sqrt{(\Delta x)^2 + (\Delta y)^2}}{2R_0}$$

where the current contact point is denoted as (x_0, y_0) , the main region of interest(ROI) for finding the next contact point is defined as the interval $x_0 < x \leq x_0 + 2R_0$, and any data points within the ROI are denoted as $(x_0 + \text{change in } x, y_0 + \text{change in } y)$.

Next, beta is calculated as:

$$\sin \beta = \cos \alpha$$

And resulting angle, which indicates the angular distance to the next contact point, can be calculated by the equation shown below (Pradipta, 2015):

$$\delta = \sin^{-1} \left[\frac{\sqrt{(\Delta x)^2 + (\Delta y)^2}}{2R_0} \right] - \tan^{-1} \left[\frac{\Delta y}{\Delta x} \right]$$

3. Identification of successive contact points: By recognizing the delta, we can easily determine all subsequent contact points from the data. Starting with the first data in the dataset as the initial contact point, we determine the direction in which the imaginary wheel rotates and identify the subsequent contact points that will be touched by the wheel. The point reached by the minimum rotation Angle delta will be regarded as the next contact point.

4. Validation and Adjustment of Data Points: All contact points are compared with the original data, and the outliers are identified and excluded to accurately reveal the general pattern of TEC variation in the ionosphere without the influence of noise. Then, pointing out the contact points in the image (red) (Picture a in Figure 2.3), connecting dots into a line (Picture C in Figure 2.3), and setting a 10% envelope to include more detail of data (Picture B in Figure 2.3). This is a crucial step to reduce the error in the final data.

3.3 Data Analysis and Modeling

Understanding the relation between Local solar time (LST) and TEC is essential to delineating how the temporal dynamics influence the dayside and nightside ionosphere. In addition, LST serves as an optimal parameter to distinguish the dayside and nightside ionosphere, providing a precise temporal framework to assess how variations in solar exposure impact the ionospheric electron density. This temporal segmentation allows us to evaluate TEC fluctuations across different LST intervals, thereby enhancing the analysis of the variation of TEC at different times. Typically, we define and distinguish the dayside

ionosphere and nightside ionosphere by the amount of direct incidence of solar radiation. By such criteria, we define that 6:00 to 18:00 is the dayside and the rest as the nightside, and the time near and before 18:00 is considered as dusk on mars.

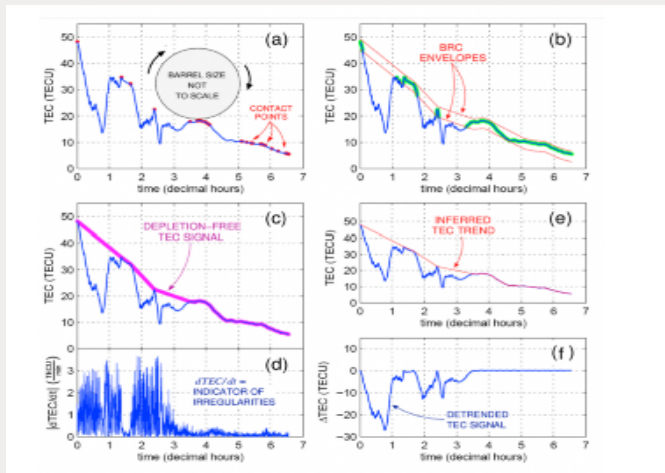


Figure 2.3: This picture shows the processes of processing the data by using the rolling barrel algorithm. We can easily understand how the rolling barrel algorithm works as a wheel rolls on the data line and when the barrel faces the valley it can cross the valley instead down to the bottom of the valley and then up. Also, we can see we use 10% envelope to contain more useful information (data points)(Rezy Pradipta, 2015)

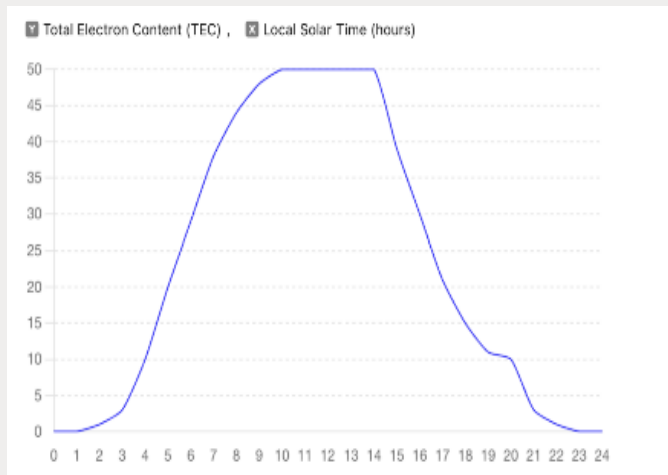


Figure 3.1: This graph reflects the change of TEC with the changing of the local solar time (LST). It not only prints out every change of the nightside ionosphere's TEC but also the dayside ionosphere's TEC. This graph combines with not just a day's data instead it combines with thousands of data sets.

In Figure 3.1, the diurnal variation of the TEC is depicted, showing a manifest increase in TEC starting around 3 AM, reaching its peak at 10 AM. After 10 AM until 13 AM, TEC remains elevated and forms a plateau at its peak. Following sunset with decreased solar radiation and thus the weakening of ionization and excitation reactions, the electrons produced in

the daytime will recombine with the positive ions, leading to a decrease in the TEC value. Therefore, the TEC value experiences a steady decline after 3 PM. Additionally, the meager Martian atmosphere and weak magnetic field enable gas molecules to escape into space, which in turn impact the TEC content within the nightside ionosphere. Finally, at midnight about 23:00 to 1:00, the TEC will reach its minimum value of the day. Such a cyclic pattern reflects the periodic nature of TEC variation driven by the solar radiation cycle.

However, the real Martian ionosphere exhibits more complex and variable behaviors that are not shown in Figure 1, which I have already smoothed. In addition to the normal diurnal response of the Martian ionosphere driven by solar radiation, both the dayside and nightside ionosphere are subjected to a wide variety of abnormal events, particularly on the nightside ionosphere. For example, on the night side of Mars, the ionosphere is usually thinner, but in some cases, it can be abnormally enhanced due to collisions of high-energy particles or the thermoelectric ionization effect (Gurnett et al., 2008). Consequently, given the sharp increase in optical thickness caused by dust storms, the penetration depth of extreme ultraviolet radiation will be significantly reduced, which will result in reduced electron density of the M2 layer during Martian global dust storms and the upward shifting of the ionospheric height (Withers & Mendillo, 2005).

The final data, refined with the algorithm of the rolling barrel, was compared with the unprocessed baseline data to figure out the abnormal parts of the Martian original data, enabling the identification of anomalous deviations within the Martian ionosphere. By systematically isolating these irregularities, we can facilitate the study of the underlying factors contributing to the atypical ionosphere behavior. Data in Figure 3.2, which has already been refined by the algorithm of the rolling barrel, illustrates the variation of TEC value with respect to Local Solar Time (LST). The data reveals the abnormal TEC fluctuation at the nighttime ionosphere where TEC value frequently drops below zero, compared with that in the dayside ionosphere where TEC increases more rapidly and maintains at a higher level.

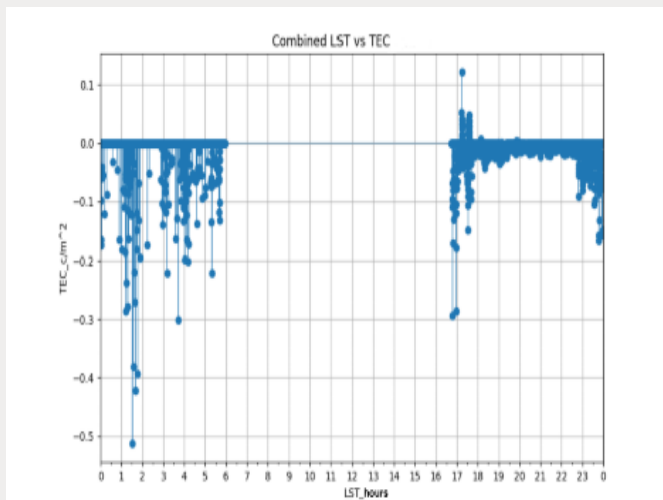


Figure 3.2: Combined Local Solar Time (LST) vs Total Electron Content (TEC) at the nightside Martian ionosphere.

Figure 3.3 presents the frequency of non-zero TEC occurrence per hour in the Martian nightside ionosphere per hour in a day. The data clearly demonstrate that abnormal ionospheric actions predominantly occur during the nighttime and dusk hours, with peak frequencies observed around 0:00, 1:00, and 23:00 LST. This illustrates the heightened activity and variability in the ionosphere during the period without direct solar radiation. Notably, this graph integrates data from multiple datasets, thereby capable of comprehensively reflecting the abnormal actions in the nightside ionosphere. In Figure 3.4, the graph shows the abnormal actions during the different Solar Zenith Angle (SZA), revealing how electron density varies under different illumination conditions. As SZA increases, moving toward the terminator and beyond into the nightside, the TEC frequency drops to negative values, highlighting abnormal electron density depletions during low solar elevation angles at the nightside ionosphere.

Figure 3.5 displays the frequency of non-zero TEC occurrences across different SZA intervals, providing insight into how TEC abnormalities distribute relative to solar position. The highest frequency of non-zero TEC values occur at the smallest SZA ranges. As the SZA increases, representing deeper nightside conditions, the incidence of non-zero TEC diminishes significantly. This pattern shows the sensitivity of the Martian ionosphere to solar radiation and drastic variability under low-light conditions, highlighting the complex interplay between SZA and electron density dynamics.

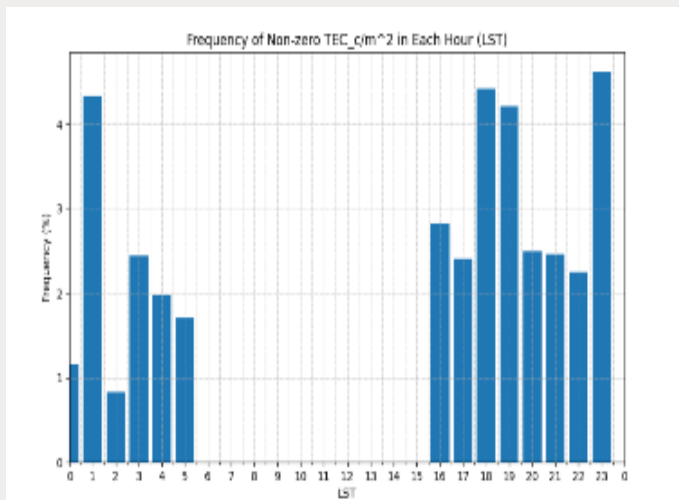


Figure 3.3: The graph shows the frequency of abnormal actions in the martian nightside ionosphere (including dusk) per hour in a day. This graph has already combined with many

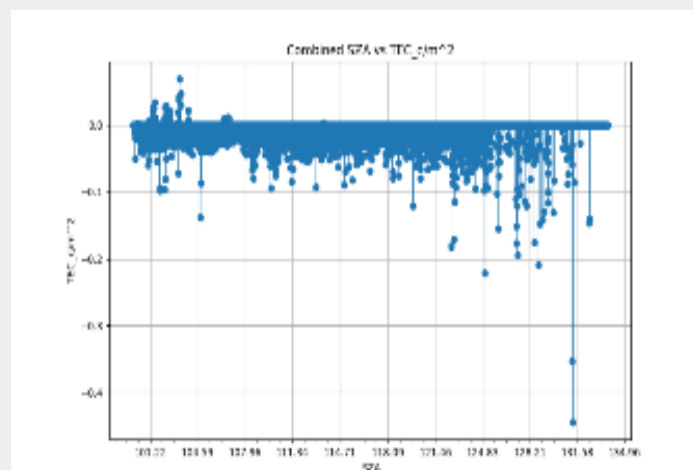


Figure 3.4: The graph clearly shows every abnormal action during the different Solar Zenith Angle (SZA). It combines with a large data set with thousands of files, therefore it is representative.

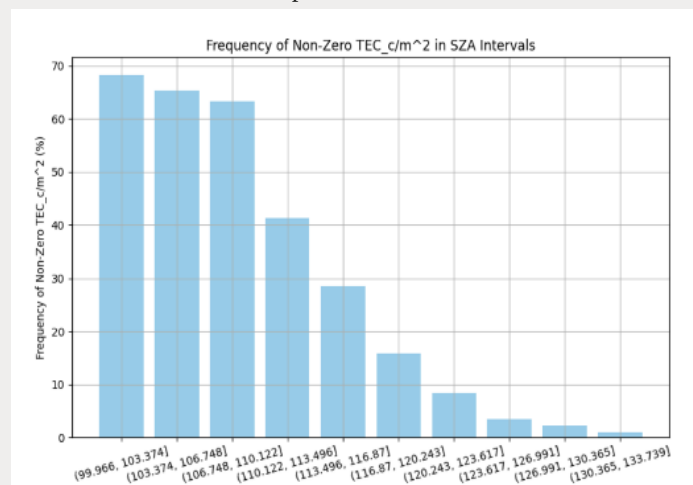


Figure 3.5: The graph reflects the abnormal action occurrence rate in every period of the SZA. We can observe the TEC change trend when the SZA changes in the nightside ionosphere.

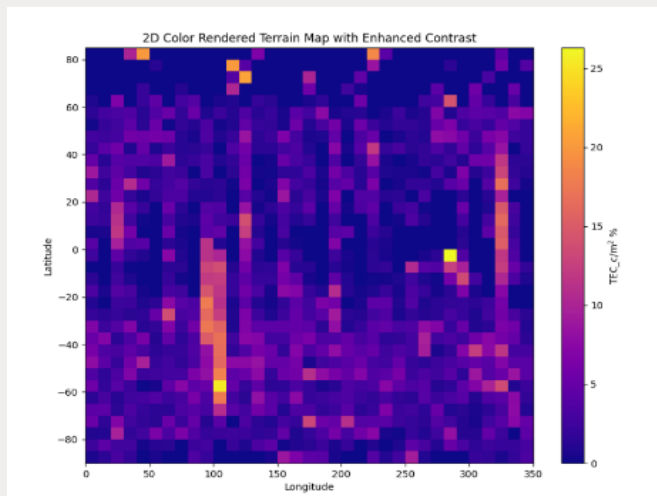


Figure 3.6: 2D Color Rendered Terrain Map clearly shows the frequency of the nightside ionosphere's abnormal action in different locations in the Mars (longitude and latitude). It synthesizes many data from Mars Express, instead not just one day data.

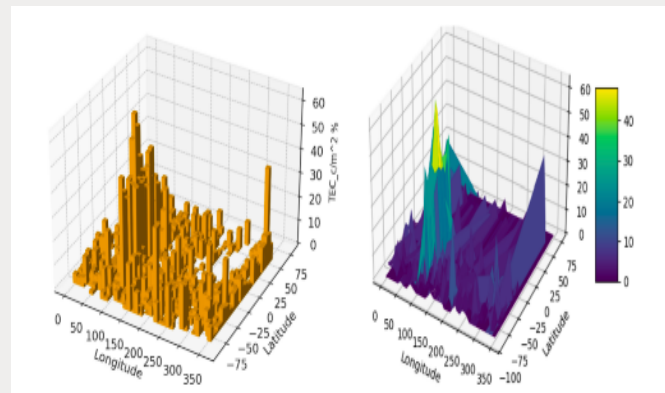


Figure 3.7: Both two graphs are 3D Color Rendered Terrain Maps which make the data visualized to help to comprehend and analyze the data.

Upon examining Figure 3.6 and Figure 3.7, it is evident that the distribution of frequency of the abnormal TEC actions is uneven. Such uneven patterns suggest complicated underlying mechanisms influencing the ionosphere behavior. As highlighted in the introduction, these reactions increase the electrical conductivity in the ionosphere, directly contributing to the increase in TEC. Enhanced electrical conductivity is usually correlated with an increase in the ionospheric electron density, leading to localized change in ionospheric structure and thus in significant shift in electron density distribution, particularly in high-conductivity regions. This relationship underscores the critical link between conductivity, electron density, and TEC variation, providing further validation of the observed anomalies and enhancing our understanding of ionospheric dynamics on Mars.

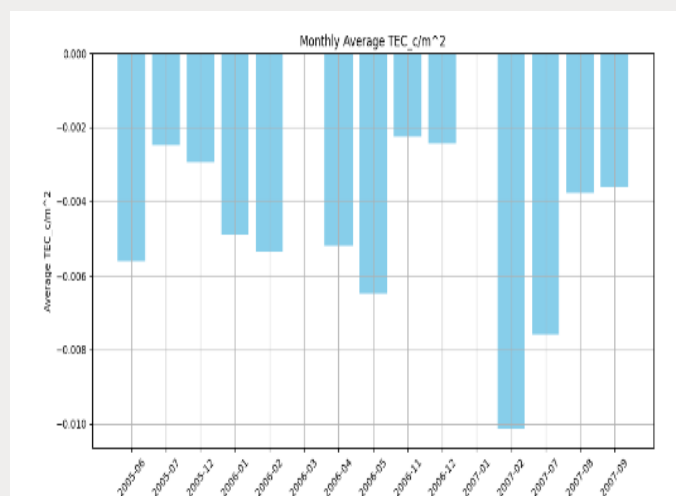


Figure 3.8: This graph shows the monthly abnormal actions of TEC of the martian nightside ionosphere in the different time of Julian calendar (it has already turned into the time of UTC). Because the datas' time is at night, there are some places without data.

An analysis of Figure 3.8 reveals that when comparing the 2005-06 with early 2006, although the TEC continues to decrease, the trend from 2005-06 to 2005-07 is increasing. Referring to the graph of solar radiation in 2005 Figure 3.10, it is evident that the solar radiation levels increased from 2005-06 to 2005-07. Further comparison made between the 2005-07 and 2005-12 data shows a more pronounced decline in TEC, aligning with the reduced solar radiation we observe in the same period. The 2006-01 shows a significant decrease in TEC compared to 2005-12 in the Figure 3.8, which corresponds to a marked reduction in solar radiation as depicted in Figure 10. Additionally, we compare the 2006-04 with the 2006-05, where 2006-04's solar radiation exceeds that of 2006-05, yet May displays a trend of deceleration in TEC reduction, suggesting an inverse relationship between solar activity and ionosphere density dynamics. As a result, based on the analysis, it is reasonable to hypothesize that most data patterns in the Martian nightside ionosphere are significantly influenced by solar activity. Increased solar radiation reaching Mars is expected to enhance the ionization rates in the nightside ionosphere, thereby elevating the TEC. As solar radiation intensifies, the nightside ionization exhibits a corresponding upward trend, thereby increasing TEC values in the Martian nightside ionosphere. However, as revisiting the graph, it is clear that even though some change of the nightside Martian nightside ionosphere aligns with the hypothesis mentioned above, the real situation is far more complex and influenced by the

and influenced by the interplay of multiple factors. The variability of TEC cannot be solely attributed to solar radiation. Given this complexity, the abnormal phenomena and TEC in the martian nightside ionosphere cannot be comprehensively explained by one or two factors alone, and therefore, a multi-factorial approach is essential to validate meaningful conclusions from the observed data.

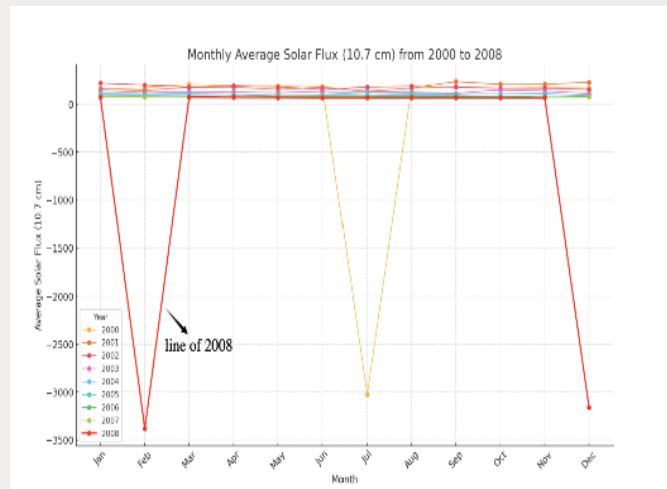


Figure 3.9: The graph is a comprehensive graph that combines the daily data of solar radiation from 2000 to 2008. In this graph, we can easily observe the change of the strength of the solar radiation. Although most of the lines of the data look like they do not have a big change, it is actually because there are some large solar actions are occurred during the 2000-2008.

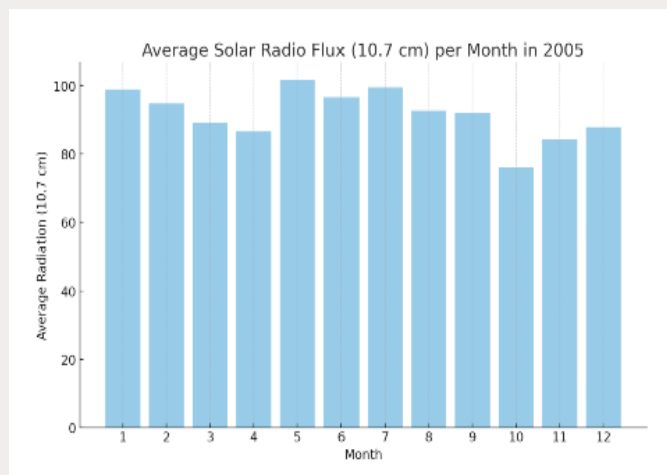


Figure 3.10: The graph shows the solar radiation strengthen per month in 2005.

As one of the most topographically diverse planets in the solar system, Mars exhibits a rich array of features on its surface, from towering volcanoes to deep canyons, vast plains, to vast basins. These topographic features not only define the geological history of Mars, but also have important effects on the Martian atmosphere and ionosphere. One of the most striking topographic features on Mars is its volcanoes and plateaus.

Olympus Mons is the highest volcano in the solar system, reaching a height of about 22 kilometers and a diameter of about 600 kilometers. This massive shield volcano is not only a geological wonder, it has also had a profound effect on the movement of the Martian atmosphere. Another notable topographic feature is Mars' Tharsis Plateau, which is home to several large volcanoes, including Mount Olympus. The formation of these volcanic groups is closely related to the thermal activity in the interior of Mars, and plays an important role in the flow and heat transport of the surface atmosphere.

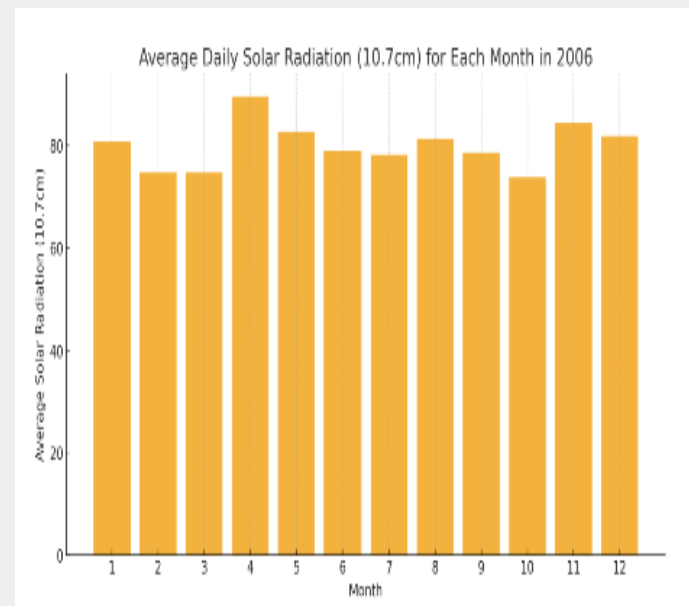


Figure 3.11: The graph show the solar radiation strengthen per month in 2006.

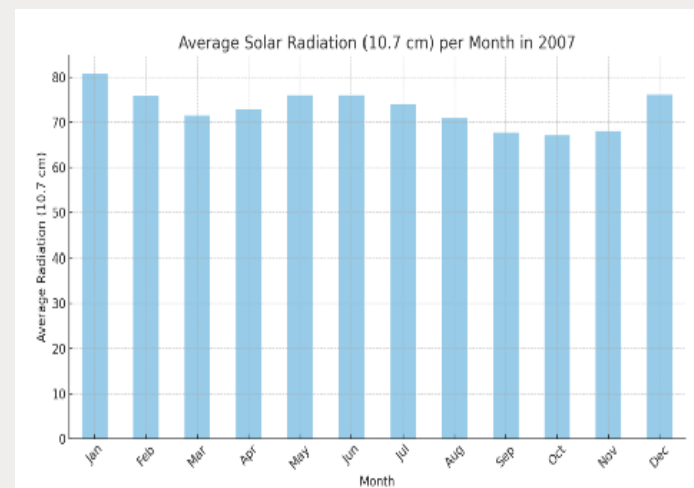


Figure 3.12: The graph show the solar radiation strengthen per month in 2007.

The surface of Mars also hosts some large impact basin and canyon systems. Hellas Basin, a massive impact crater about 2,300 kilometers across and more than 7 kilometers deep, is one of the most significant

topographic features in the southern hemisphere of Mars. Valles Marineris is the largest canyon system in the solar system, with a length of about 4,000 km and a depth of up to 7 km. The formation of this canyon system is associated with the breaking and spreading of the Martian crust, which has had a significant impact on the interaction of the Martian surface and atmosphere. Valles Marineris is the largest canyon system in the solar system, with a length of about 4,000 km and a depth of up to 7 km. The formation of this canyon system is associated with the breaking and spreading of the Martian crust, which has had a significant impact on the interaction of the Martian surface and atmosphere.

Mars also has vast plains and sand dunes. The Northern Plains, which covers much of the northern hemisphere of Mars, presents relatively flat and young features. These plains may have been the result of ancient Marine or glacial processes. The Southern Highlands, the dominant topographic feature in the southern hemisphere of Mars, is riddled with ancient impact craters, indicating a complex geological history.

The poles of Mars are covered with polar ice caps made up of dry ice and water ice. The Arctic ice sheet partially melts in the summer, while the Antarctic ice sheet is more stable. These polar ice caps have important effects on Mars' climate and seasonal changes.

Plateaus and volcanoes can affect the flow of the atmosphere and create local climatic phenomena. Canyons and basins affect atmospheric pressure and temperature, resulting in unique meteorological conditions. These topographic features work together to shape Mars' unique environment and also have a significant impact on the dynamic behavior of its atmosphere and ionosphere.

The topographic influence is also an important factor to the martian nightside ionosphere. The topography of mars impacts the martian nightside ionosphere in many ways like other factors. First is the effect of topographic elevation on atmospheric density. Topographic fluctuations not only change local air pressure and flow patterns, but also affect the overall structure and composition of the atmosphere. It will impact the TEC and the abnormal actions of the martian nightside ionosphere from pressure

differences and atmospheric density, air flow patterns, air temperature, atmospheric circulation. As for the air pressure differences and atmospheric density, they are inextricable. We divide the air pressure into highland air pressure and lowland pressure.

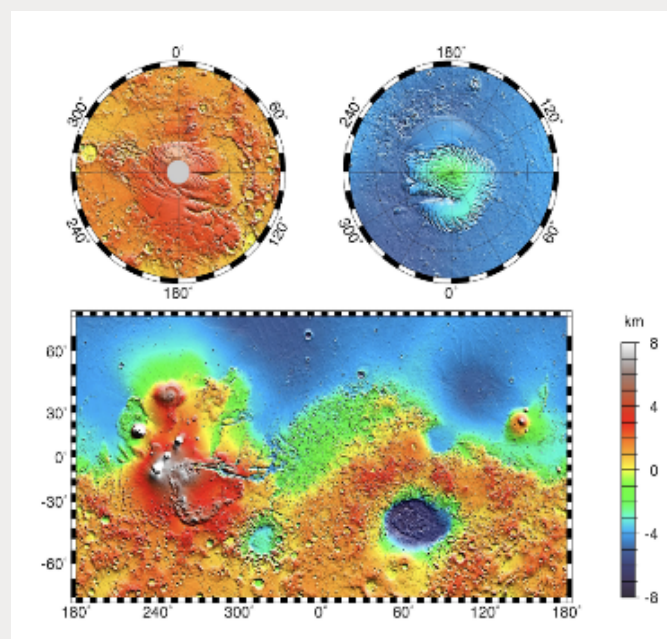


Figure 3.13 : This is the global topographic map of Mars. The global topographic maps of Mars use Mercator projections up to 70° latitude and stereographic projections for the poles, with the south pole on the left and the north pole on the right.

These maps highlight the significant elevation differences between Mars' northern and southern hemispheres. The Tharsis volcanic region, positioned near the equator within longitudes 220° E to 300° E, includes the extensive Valles Marineris canyon system stretching east-west. This region also features several major volcanic mountains such as Olympus Mons (located at 18° N, 225° E), Alba Patera (42° N, 252° E), Ascraeus Mons (12° N, 248° E), Pavonis Mons (0°, 247° E), and Arsia Mons (9° S, 239° E).

On Mars, highland areas such as Tharsis Plateau and Olympus Mons have relatively low air pressure due to their high elevation. This is because the air pressure decreases with altitude. According to the basic physical properties of gases, the air pressure is directly related to the height of the gas. The lower pressure in the highlands results in a significant decrease in atmospheric density in the region. The lower pressure reduces the frequency of collisions between gas molecules, which affects the formation of electrons and ions in the ionosphere.

In contrast to the highlands, low-lying regions on Mars such as the Heras Basin and the Northern Lowlands have relatively high air pressure due to their low topography.

In these lowland areas, the gas density is higher due to the higher pressure. This leads to an increased frequency of collisions between gas molecules, which increases the concentration of electrons and ions in the ionosphere. Regions of high atmospheric pressure usually exhibit higher atmospheric density, and this increased density can increase the overall ionization rate of the atmosphere.

Another factor is airflow pattern. The terrain guides the air currents on Mars, since the ups and downs of the terrain can have a significant effect on air flow. On Mars, topographic features such as mountains, volcanoes, and basins change the path and speed of air currents. For example, mountains and valleys can direct the wind direction and change the way air flows. Such terrain guides air currents in a way that causes air currents to shift between different regions, affecting the density of the atmosphere in those regions.

Topographic features of the Martian surface can also cause changes in wind speed and direction. In high areas, due to the relief of the terrain, the air is forced to rise and form an updraft. In low-lying areas, downdrafts form. Changes in these winds can affect the mixing and distribution of gases, further altering local atmospheric density. For example, topographic changes caused by volcanic eruptions or seismic activity can trigger local air flow changes that alter the distribution of gases and thus affect atmospheric density.

To be more specific, the high ground usually forces the air up, while the low ground guides the air down. These air currents vary particularly significantly during the day and night, with the cooling effect being more pronounced at night, resulting in distinct patterns of rise and fall in the night-side ionosphere. Topographic features such as canyons (such as Marina Canyon) and mountains on the Martian surface create local wind fields that change the speed and direction of air currents. For example, when the air stream encounters a canyon, it is forced into the canyon, creating strong wind flow; When the air hits a mountain, it is forced up or around it. Therefore the regions in the martian nightside, their frequency of the abnormal actions of the ionosphere and the TEC of the ionosphere will be changed obviously.

Third, thermal current also influences the martian nightside ionosphere. As for the thermal current, it is large scale gas flows caused by temperature differences. On Mars, the formation of thermals is mainly related to topographic height differences and seasonal changes in polar ice caps. The topography of Mars varies significantly in height, and the temperature difference between the highlands and the lowlands creates strong thermals. For example, volcanic activity on the Tharsis plateau can cause local areas to warm up, creating rising thermals. These thermals can carry ions and electrons from the lower atmosphere to the higher levels, affecting the electron density of the ionosphere. And Mars' polar ice caps partially melt in the summer and refreeze in the winter. This seasonal change causes temperature fluctuations in the polar regions, creating strong thermals. These thermals not only affect the movement of the polar atmosphere, but also have an indirect effect on the night-side ionosphere through the global atmospheric circulation.

Thermals can transport ions and electrons from the lower atmosphere vertically to the upper ionosphere. This vertical transport is particularly significant in the highlands and volcanic regions of Mars. For example, volcanic activity on the Tharsis plateau produces strong updrafts that carry large numbers of ions and electrons to the ionosphere, increasing the local electron density. And the vertical motion of the hot gas also causes the change of local electric field. When hot gas streams transport ions and electrons vertically into the upper atmosphere, charge separation forms, leading to the establishment and change of electric fields. This electric field change will further affect the trajectory and distribution of electrons, thus changing the electron density in the ionosphere. The influence of current on the ionosphere is mainly realized through electromagnetic action and the heating effect that I write in this article above.

The differences of temperature will also contribute to the abnormal actions of the nightside ionosphere in the mars and change of TEC. These temperature differences are mainly achieved through thermodynamic processes and atmospheric dynamics. Variations in the topography of the Martian surface result in different thermodynamic properties in different regions. For example, highlands such as Tharsis Plateau and Mount Olympus receive less solar radiation due to their high

altitude, so these areas are relatively cold. Conversely, lowlands such as the Heras Basin, due to their low location, are able to receive and retain more solar heat, so these areas are relatively warm.

These temperature differences are particularly pronounced on the night side of Mars. During the day, the surface of Mars absorbs solar radiation, causing temperatures to rise. At night, the surface of Mars radiates heat, but due to different terrain characteristics, the heat dissipation rate is different, the heat dissipation rate is faster in the highlands, and the heat dissipation is slower in the lowlands, resulting in a further increase in the night temperature difference.

In the Figure 3.13, we can see that at about 220 degrees to 300 degrees east, about 45 degrees north to 45 degrees south, there is a concentrated area of high overall height, and that's because the Tharsis volcanic region, positioned near the equator within longitudes 220° E to 300° E and the Olympus Mons (located at 18° N, 225° E), Alba Patera (42° N, 252° E), Ascraeus Mons (12° N, 248° E), Pavonis Mons (0°, 247° E) all of them are in the region from about 220 degrees to 300 degrees east. At about 50 degrees east longitude to about 110 degrees south latitude, a basin area appears that is significantly lower than all surrounding areas. In Figure 3.6, we can observe that in the areas mentioned above the phenomenon is similar to what I say in the passages above. In order to help to comprehend, I combine the Figure 3.13 and Figure 3.6, and box the area I'm talking about. Figure 3.14 is on the next page (the passages below will use the region 1, region 2, region 3, region 4 in Figure 3.14 to represent the highland and the lowland just said).

According the passages above, I guess in the Figure 3.14 the region 1 will has a low electron density (TEC) and then its frequency of the abnormal actions of TEC in the martian nightside ionosphere is low, instead in the Figure 3.14 the region 2 will has a high electron density (TEC) and then its frequency of the abnormal actions of TEC in the martian nightside ionosphere is high. Because region 1 in the Figure 3.14 is the highland that is higher than the regions which are near it and the region 2 in the Figure 3.14 is the lowland that is much lower than any other regions in the mars.

In Figure 3.14, the frequency of the region 3 abnormal actions of TEC in the martian nightside ionosphere is higher than surrounding areas. Besides, the places in region 3 are not like other places where most of the high frequency places are dispersive, those places are concentrated and obvious. It is fit for what I guess. In the region 4 in Figure 3.14, most of the places' frequency of the abnormal actions of TEC in the martian nightside ionosphere is low. It seems like my guess is correct, but actually region 4 still has some places with high frequency. This is because the vertical transport of thermal current and it can transport ions and electrons from the lower atmosphere vertically up into the ionosphere. Besides, this vertical transport is particularly significant in the highlands and volcanic regions of Mars. According to the passage above we can know the Tharsis plateau is in there. Volcanic activity on the Tharsis Plateau produces strong updrafts that carry large numbers of ions and electrons to the ionosphere, increasing the local electron density. Therefore we can see that that region has some places quite different from the other places, they have high density of electrons (TEC) like region 3. All the processes here are also involved and driven by temperature differences, whether it's high density in the lowlands, low density in the highlands, or thermals.

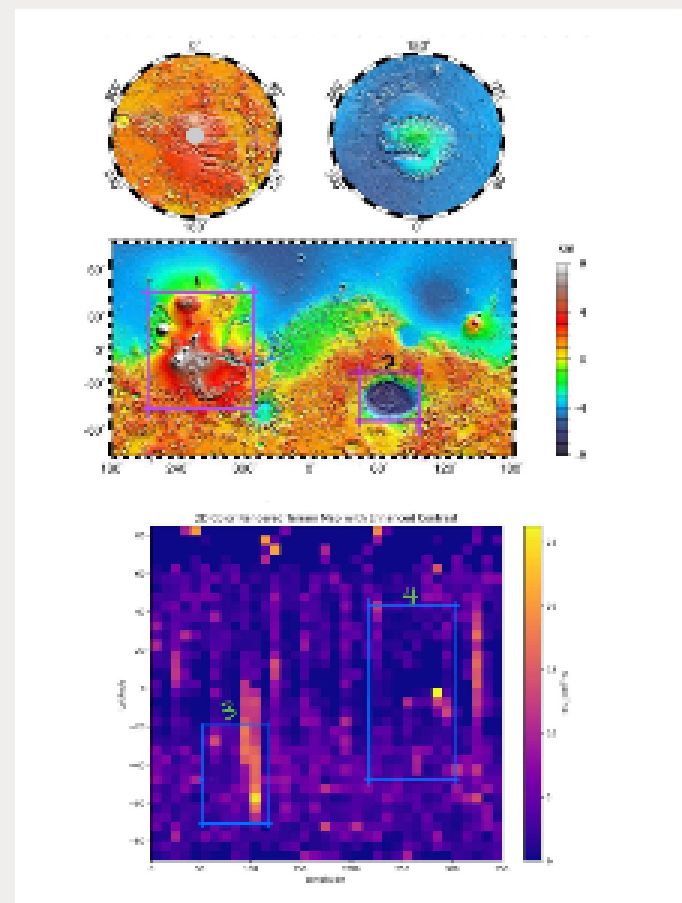


Figure 3.14: Region 1 is the highland I say in the passage above, and region 2 is the lowland I say in the passage above. Both of them are the topographic map. Regions of 3 and 4 are corresponding to regions of 2 and 1 respectively. Regions of 3 and 4 reflect the frequency of the nightside ionosphere's abnormal action in different locations in the Mars (longitude and latitude).

4. Conclusion

In conclusion, the effect of Martian topography on the electron density of the night side ionosphere is a complex and multifaceted process. These effects are mainly achieved by changing atmospheric density, thermodynamic processes and atmospheric motion. Through detailed analysis of these mechanisms and their essential causes, this paper reveals how Martian topography changes affect the electron density of the night side ionosphere.

First, the topography of the Martian surface directly affects the density and structure of the atmosphere. In higher regions (such as Tharsis and Olympus), the atmosphere is thinner due to lower air pressure. This thin atmosphere reduces the frequency of collisions between gas molecules, which reduces the production rate of electrons and ions in the ionosphere. Specifically, in the highland regions of Mars, the density of atmospheric molecules is reduced due to low atmospheric pressure, which means that the number of gas molecules that can be ionized when the solar wind and cosmic rays reach these regions is reduced, resulting in relatively low ionospheric electron density in these regions.

In contrast, in the lowland regions of Mars, such as the Heras Basin and the Northern Lowlands, the pressure is higher, resulting in a thicker atmosphere. This higher atmospheric density increases the collision frequency of gas molecules, which increases the production rate of electrons and ions, resulting in an increase in ionospheric electron density. For example, the depth and topography of the Heras Basin, one of the largest impact basins on Mars, make the atmosphere thicker in this region, which in turn produces more electrons and ions under the action of solar radiation, increasing the electron density of the night-side ionosphere.

Second, Martian topography further influences ionospheric electron density through thermodynamic processes and atmospheric motion. Highland and volcanic regions produce strong updrafts that can carry ions and electrons from the lower atmosphere to the higher ionosphere, altering the distribution of electron density. For example, volcanic activity on the Tharsis plateau can lead to strong currents that not only carry lower atmospheric material to higher levels, but may also carry ions and electrons from the ionosphere, creating regions of high electron density high in the sky. This phenomenon is not only common on Mars, but has also been observed in similar topographic regions on Earth, indicating the profound influence of topography on atmospheric motion and ionospheric structure.

The complex topography of Mars also affects the distribution of ions and electrons in the ionosphere by directing and altering the wind field in the atmosphere. Topographic features such as canyons and basins create unique local wind fields that can create regions of high electron density in the night-side ionosphere. For example, Marina Canyon is the largest canyon system in the Solar system, and its depth and width significantly affect the airflow in this region, forming a unique wind field structure. These wind fields not only affect the climate and meteorological conditions inside the canyon, but also alter the distribution of electrons in the ionosphere above the region.

In addition, variations in Martian topography affect ionospheric electron density through thermals generated by temperature differences. The temperature difference between high and low ground can create strong thermals that can change the electric and magnetic fields in the ionosphere, affecting the distribution of electrons. For example, in the polar regions of Mars, the melting and freezing processes of the polar ice caps produce strong seasonal thermals as the seasons change. These hot gases not only affect the atmospheric circulation in the polar regions, but also affect the electron density distribution of the night side ionosphere by changing the electric field structure in the ionosphere.

The current change caused by the hot gas flow also has a significant effect on the ionospheric electron density.

The presence of hot gas leads to current changes in the ionosphere, and these current changes further alter the electric field structure, thus affecting the movement and distribution of electrons. Specifically, as thermals move through the atmosphere, they generate local currents that affect the distribution of electric fields in the ionosphere. Changes in the electric field guide the movement of electrons, causing them to accumulate in certain regions, thus forming regions of high electron density. This phenomenon is particularly pronounced in Martian canyons, basins, and polar regions, indicating the profound influence of topography and thermodynamic processes on electron density in the ionosphere.

In summary, the topography of Mars has a significant effect on the electron density of the nightside ionosphere by altering atmospheric density, thermodynamic processes, and atmospheric motion. The higher regions have lower electron density due to the thinner atmosphere. The lower regions have higher electron density due to the thicker atmosphere. In addition, thermodynamic processes such as updrafts, local wind fields and thermals caused by volcanic activities and topographic changes also affect the generation and distribution of electrons in the ionosphere to a certain extent. The essential reason for these effects lies in the changes of atmospheric and electromagnetic environment caused by terrain changes, which in turn affect the production and distribution of electrons in the ionosphere.

5. Works Cited

- Ionosphere | NOAA / NWS Space Weather Prediction Center (n.d.-a). <https://www.swpc.noaa.gov/phenomena/ionosphere>
- Juan, J. M., Sanz, J., Rovira-Garcia, A., González-Casado, G., Ibáñez, D., & Perez, R. O. (2018). AATR an ionospheric activity indicator specifically based on GNSS measurements. *Journal of Space Weather and Space Climate*, 8, A14. <https://doi.org/10.1051/swsc/2017044>
- Peter, K., Sánchez-Cano, B., Němec, F., González-Galindo, F., Kopf, A. J., Lester, M., Pätzold, M., Regan, C. E., & Holmström, M. (2024). The Ionosphere of Mars After 20 Years of Mars Express Contributions. *Space Science Reviews*, 220(4). <https://doi.org/10.1007/s11214-024-01078-x>
- Withers, P. & Center for Space Physics, Boston University. (2009). A review of observed variability in the dayside ionosphere of Mars. In *Advances in Space Research* (Vols. 44–44, pp. 277–307) [Journal-article]. <https://doi.org/10.1016/j.asr.2009.04.027>
- Pradipta, R., Valladares, C. E., & Doherty, P. H. (2015). An effective TEC data detrending method for the study of equatorial plasma bubbles and traveling ionospheric disturbances. *Journal of Geophysical Research Space Physics*, 120(12). <https://doi.org/10.1002/2015ja021723>
- Total Electron Content | NOAA / NWS Space Weather Prediction Center. (n.d.). [https://www.swpc.noaa.gov/phenomena/total-electron-content#:~:text=The%20Total%20Electron%20Content%20\(TEC,radio%20signal%20will%20be%20affected](https://www.swpc.noaa.gov/phenomena/total-electron-content#:~:text=The%20Total%20Electron%20Content%20(TEC,radio%20signal%20will%20be%20affected)
- Hook, S. (n.d.). JPL Science: MARSIS. <https://science.jpl.nasa.gov/projects/marsis/#:~:text=The%20main%20objective%20of%20MARSIS,studies%20over%20the%20entire%20planet>
- Pradipta, R., Valladares, C. E., & Doherty, P. H. (2015b). An effective TEC data detrending method for the study of equatorial plasma bubbles and traveling ionospheric disturbances. *Journal of Geophysical Research Space Physics*, 120(12). <https://doi.org/10.1002/2015ja021723>
- Wang, X., Xu, X., Cui, J., Gu, H., Niu, D., Zhou, Z., Chang, Q., Xu, Q., Luo, L., He, P., & Yi, S. (2022). Electron density variability in the day-side ionosphere of Mars: The role of gravity waves. *Monthly Notices of the Royal Astronomical Society*, 518(3), 4310–4321. <https://doi.org/10.1093/mnras/stac3396>
- Cao, Y., Cui, J., Wu, X., Guo, J., & Wei, Y. (2019). Structural Variability of the Nightside Martian Ionosphere Near the Terminator: Implications on Plasma Sources. *Journal of Geophysical Research Planets*, 124(6), 1495–1511. <https://doi.org/10.1029/2019je005970>
- Peter, K., Sánchez-Cano, B., Němec, F., González-Galindo, F., Kopf, A. J., Lester, M., Pätzold, M., Regan, C. E., & Holmström, M. (2024b). The Ionosphere of Mars After 20 Years of Mars Express Contributions. *Space Science Reviews*, 220(4). <https://doi.org/10.1007/s11214-024-01078-x>
- Krasnopolsky, V. A. (2019). Spectroscopy and Photochemistry of Planetary Atmospheres and Ionospheres. <https://doi.org/10.1017/9781316535561>
- Bougher, S. W., Pawlowski, D., Bell, J. M., Nelli, S., McDunn, T., Murphy, J. R., Chizek, M., & Ridley, A. (2015). Mars Global Ionosphere-Thermosphere Model: Solar cycle, seasonal, and diurnal variations of the Mars upper atmosphere. *Journal of Geophysical Research Planets*, 120(2), 311–342. <https://doi.org/10.1002/2014je004715>